International Journal of Studies in Advanced Education
Volume 03, Issue 7, July - 2024
ISSN (E): 2949-8945
Scholarsdigest.org

FORMATION OF SHRINKAGE POROSITY DURING SOLIDING OF STEEL

Sh. B.Tashbulatov,
Associate Professor
Tashkent State Technical University Uzbekistan
sh_tashbulatov@mail.ru

M. N. Gaybullaev,
PhD Student
Namangan Construction – Engineering Institute Uzbekistan
m.n.gaybullaev@umail.uz

I.T. Tukhtaboev,
PhD Student
Namangan Construction – Engineering Institute Uzbekistan
i.t.tuxtaboev@mail.ru

I.S. Abdukahorov,
Constructor
Namangan Cement LLC Uzbekistan
abdukahorov_2024@gmail.com

B.N. Turajonov,
Master's Student
Namangan Construction – Engineering Institute Uzbekistan
turajonov_akademik@umail.uz

Abstract
In this article, the formation of abrasion pores during the transition of metals from a liquid state to a solid state, and the effect of their formation on the quality of the casting is studied. Shrinkage pores, when the metal goes into a liquid state, there are several analyzes of the formation of shrinkage pores due to the fact that the volume of the metal in the liquid state is larger than the volume of the metal in the solid state, and it shrinks again during the cooling process.

Keywords: steel, alloy, porosity, liquid metal, furnace, liquation, shrinkage, ProCAST program.

International Journal of Studies in Advanced Education
Volume 03, Issue 7, July - 2024
ISSN (E): 2949-8945
Scholarsdigest.org

INTRODUCTION

During the transition of steel from a liquid state to a solid state, it is combined due to a decrease in volume due to an increase in density with a decrease in temperature. This volume reduction can be compensated by filling with liquid steel. If the fill is sufficient, porosity will not occur. At the end of solidification of the liquid metal, the resistance to flow increases, which leads to a decrease in high pressure and therefore to the formation of shrinkage pores. The purpose of this research paper is to compare experimental studies on shrinkage porosity with numerical results. Therefore, samples with different geometries were cast and cut along the longitudinal axis of the sample to determine the shrinkage porosity. Numerical simulation of castings was carried out using ProCAST software. Various porosity criteria and their corresponding porosity models have been used to predict the formation of shrinkage porosity in castings. Comparisons are made between various numerical and experimental results.

Materials and methods

Theoretical foundations of the formation of pores

The formation of porosity can be divided into two main categories: gas porosity and shrinkage porosity. The mechanism of formation and the shape of the porosity of both types of porosity showed significant differences.

Examination of gas porosity showed that the shape of this type of porosity is mostly spherical or sometimes elliptical. The formation of gas porosity is based on the decrease in saturation temperature for important gases [H], [N] and [O] (formation of CO) in liquid steel, which is illustrated in Figure 1. It also draws heat out of the mold along with the gas, which in turn lowers the temperature of the liquid steel and causes the enrichment of gaseous elements between the former or dendrite formations. The reason for the formation of gas porosity is related to the gas exceeding the saturation point. The spherical shape of this type of porosity is assumed to occur in the liquid state of formation or in the initial stage of solidification. Finally, it should be noted that the formation of gas porosity is not homogeneous, because the internal pore pressure is very high. Therefore, heterogeneous nucleation is preferred and therefore inclusions or uneven surfaces have been used as nucleation sites [1], [2], [3].

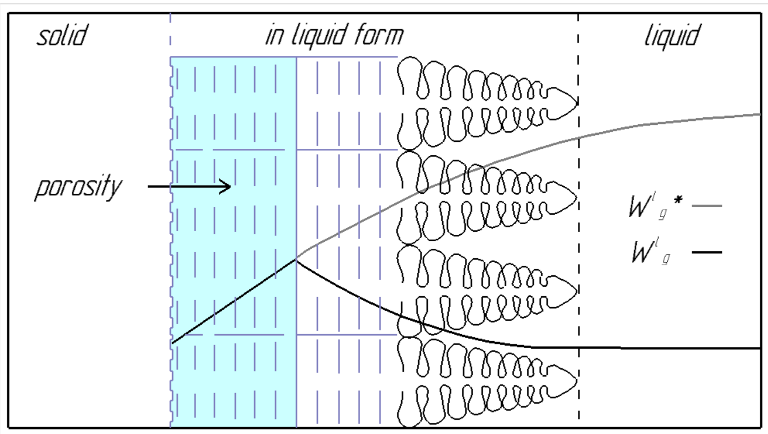

Figure 1. Schematic representation of gas concentration W^l_g increasing in the unhardened region based on gas microsegregation and decrease of solubility limit W^{l*}_g (T, p_l) [4], [5].

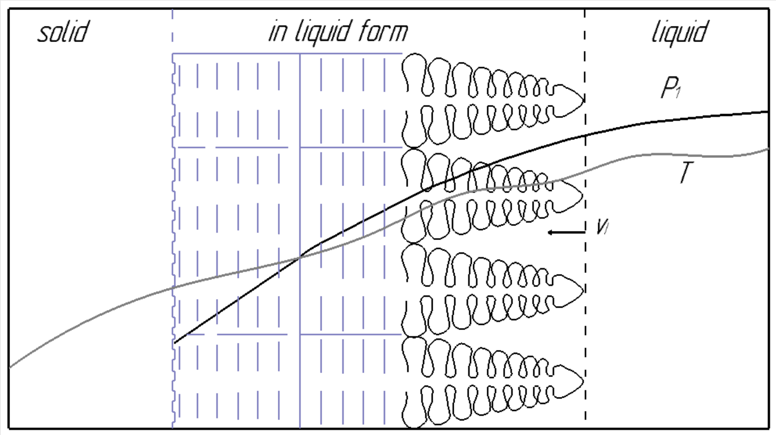

Figure 2. Schematic representation of fluid pressure drop in the unhardened region based on solidification shrinkage [6], [7].

Result and analysis

Unlike gas pores, shrinkage pores are highly tortuous in shape and are dendritic hardening alloys bounded by primary dendrites and dendrite arms. Shrinkage porosity occurs at the end of the solidification interval and therefore this type of shape is fixed by the remaining space between the dendrites. The shrinkage effect of the steel due to the decrease in temperature can be compensated by filling the liquid steel in the not yet fully solidified zone. This can be a problem for a wide range of underhardened zones, as the fluid flow of the liquid steel must be sufficient to reach the root of the dendrite. In the under – solidified zone, the restriction of fluid flow leads to a pressure drop, as shown in Fig. 2. Inadequate development of interdendritic flow reduces the pressure to a certain limit, which leads to the formation of shrinkage pores due to insufficient filling. Thus, the formation of this type of porosity can occur at the end of the solidification interval and, furthermore, the shape can occur in the remaining cavity of the dendrites. Finally, a 2D metallographic image shows only a small part of this type of porosity (around a few tens of micrometers in size) because it is usually intricately interconnected and only a 3D image can capture the full extent [8], [9]], [10].

Analysis of shrinkage porosity formation

By now, there are many ways to predict the occurrence of shrinkage porosity. These methods range from very simple methods that use only material properties or solidification parameters to very complex methods that are essentially self – programmed and attempt to explain the formation. Niyama's criterion and ProCAST's porosity algorithm were used in this work to calculate shrinkage porosity for casting. These methods are described in detail below.

Porosity criterion

[11] established a criterion for determining the appearance of shrinkage pores by Niyama et al. Therefore, they considered various easily calculated porosity criteria and compared these values with experimental results. As a result, a porosity criterion, now widely used and known as the Niyama criterion, was studied. The criterion can be calculated by the following equation (1).

$$Ny = \frac{G}{\sqrt{T}} \prec 1 \qquad (1)$$

where G – is the thermal gradient and T – is the cooling rate. For steel, the critical value is around 1.0 [(K min)$^{0.5}$/cm]. A Niyama value lower than this critical value resulted in the formation of shrinkage porosity. The advantage of this criterion is the independence of the casting geometry. However, the critical value depends on the respective casting material and must be determined for each casting material [12], [13], [14], [15].

The Niyama criterion was further developed by Carlson et al. [16]. The purpose of this refinement was to estimate not only the state of shrinkage porosity within the cast, but also the amount of pore volume. The extended Niyama criterion is also called the dimensionless Niyama criterion and can be calculated according to Equation (2).

$$Ny^* = \frac{G\lambda_2\sqrt{\Delta P_{cr}}}{\sqrt{\mu_l \beta \Delta T_f T}} = Ny\frac{\lambda_2\sqrt{\Delta P_{cr}}}{\mu_l \beta \Delta T_f} = \sqrt{I(g_{l,cr})} \qquad (2)$$

where λ_2 – secondary dendrite arm space, ΔP_{cr} – critical pressure drop; μ_l – dynamic viscosity of liquid; $\beta = (\rho_h - \rho_l)/\rho_l$ – reduction in hardening; $\Delta T_f = T_{liquid} - T_{solid}$ cooling range and $I(g_{l,cr})$ is integral, and depends on the solid – temperature curve. For simple curves, the integral can be calculated analytically by equation (3).

$$I(g_{l,cr}) = \int_{g_{l,cr}}^{1} 180\frac{(1-g_l)^2}{g_l^{\ 2}} \frac{d\theta}{dg_l} dg_l \qquad (3)$$

where $\Theta = (T - T_{solid})/\Delta T_f$ – dimensionless temperature. More details on the dimensionless Niyama criterion can be found in [17]. Carlson et al use the dimensionless Niyama criterion to understand the formation of shrinkage porosity for aluminum alloy, magnesium alloy and steel. Additional verification was performed using steel casting experience.

ProCAST's porosity model

ESI Group implemented a shrinkage porosity prediction model in ProCAST. Two important parameters are needed to calculate porosity. The first parameter is MacroFs, which corresponds to the solid fraction and defines the starting point for the porosity calculation. The second parameter is called FeedLen and can be viewed as the interdendritic fill length. Porosity calculations were performed for areas with a solids fraction between MacroFs and 1. There are two possible situations for these regions:

1. In the liquid metal – filled unsolidified zone, there are regions with a solid fraction lower than MacroFs. In this case, the distance between the solidus temperature isotherm and the MacroFs isotherm was calculated. The distance between these isotherms must be greater than FeedLen for porosity to occur. Therefore, a higher temperature gradient led to a smaller distance and vice versa, schematically shown in Figure 3. In region A, the temperature gradient is low and therefore the distance between the two isotherms is greater than FeedLen. Porosity has formed in this area. In zone B, the distance is smaller because the gradient is much higher and as a result no porosity is formed [18].

International Journal of Studies in Advanced Education
Volume 03, Issue 7, July - 2024
ISSN (E): 2949-8945
Scholarsdigest.org

2. The solid fraction of all elements in the liquid metal – filled unsolidified zone is greater than or equal to MakroF. The contraction that occurs between the macroF and the solidus temperature is compensated by the formation of porosity throughout the region [19].

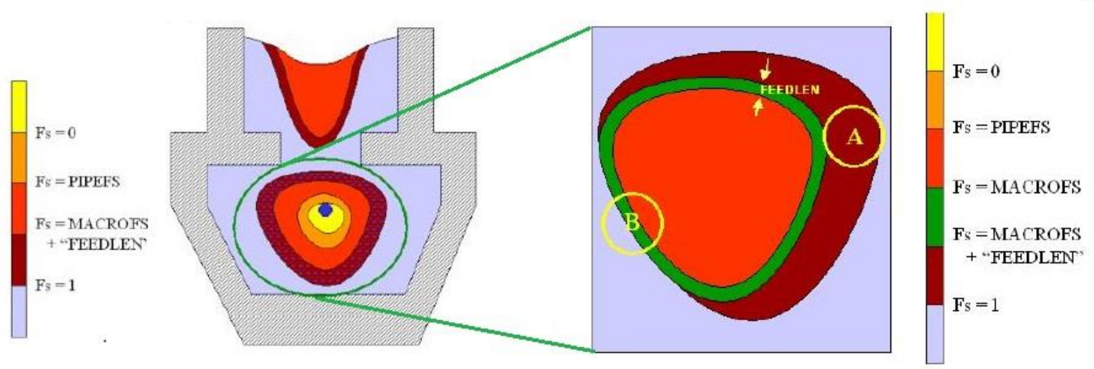

Figure 3. Schematic representation of internal shrinkage porosity calculation from ProCAST [20].

Development of experimental pouring tests

Casting tests were carried out in the melting shop at the "Foundry Shop". Thus, the mold geometries were varied to determine whether they had an effect on porosity formation.

Discussion

A filler allowance is placed at the top of the casting to influence the solidification behavior in this region. It should also be noted that the mold is not completely filled with liquid steel. The liquid steel should be approximately 30 mm below the top edge of the mold. So the dimensions of the casting are 100mm x 100mm x 370mm and the weight is around 27 kg. For better separation, the inner surface of the mold is coated with release agents. The mold is set in sand for better stability. Three experimental tests were conducted with variable taper angles varying from 0° to 5° and 10° for a thin-walled mold wall only. The wider mold side is parallel, and the mold is not preheated before casting. At the end of the casting experiment, the upper part of the sample is covered with insulating powder. The steel is cast into a mold using the overhead casting method.

The formation of shrinkage pores depends on the material. A material with a wide liquid metal under-solidification zone tends to form porosity as a material with a narrow under – solidification zone. Thus, high – carbon steel was used as the casting material. The composition of cast steel is shown in Table 1. General structural steel was used for the formwork.

Table 1 Cast steel composition

	C, %	Si, %	Mn, %	Al, %
Cast material	0.85	0.30	1.00	0.04

An important part of metallographic investigations is the determination of shrinkage porosity. For this purpose, a 10 mm piece was cut from the center of the casting. A macroscopic image was taken to identify the porosity in the center of the ingot.
The primary structure of cast samples with a mold taper of 0°, 5° and 10° is shown in Fig. 4. Shrinkage pores are highlighted in green in this image.

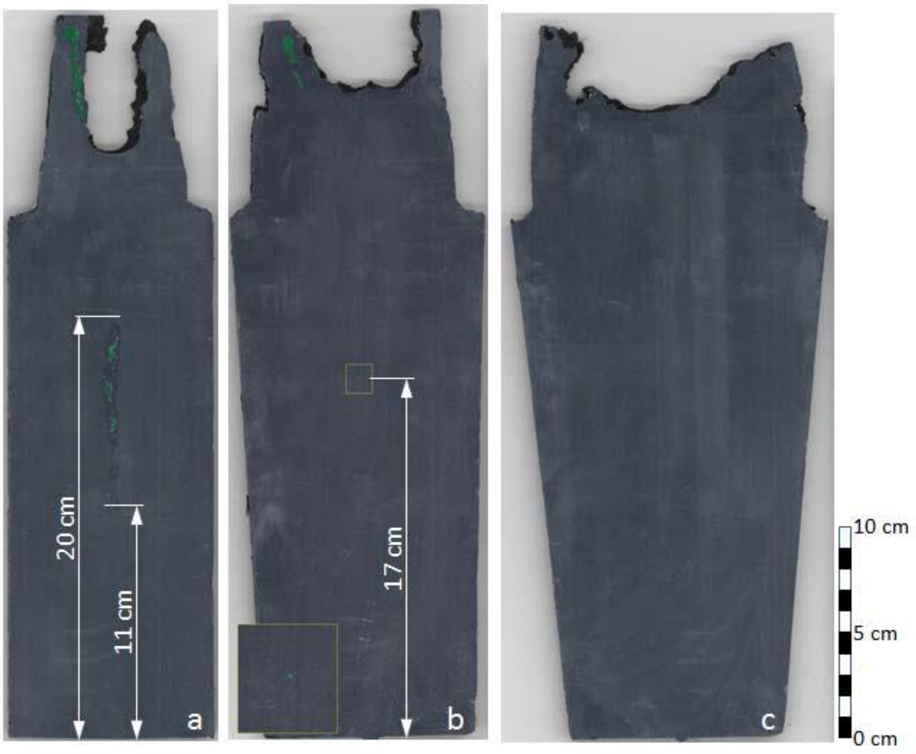

Figure 4. Experimental results of cast samples (a: 0° taper; b: 5° taper; c: 10° taper).

Conclusion

On the left is a cast without a taper. As can be seen from the figure, a shrinkage cavity appears in the center of the casting and the casting height extends from 11 cm to 20 cm. A small hole of 17 cm is determined for a 5° taper casting. A 10° taper casting was obtained without shrinkage porosity. It is also clear to see how the tube geometry changes with the die taper. Compared to a non – conical casting, the pipe has formed a very deep hole. However, this has changed to a flatter and wider tube with a higher angle of the die.

REFERENCES:

[1] Dantzig J A and Rappaz M 2009 Solidification (Lausanne: EPLF Press).
[2] Couturier G and Rappaz M 2006 Model. Simul. Mater. Sc. 253 – 71.
[3] Couturier G and Rappaz M 2006 Modeling of porosity formation in multicomponent alloys in the presence of several dissolved gases and volatile solute elements Symp. on Simulation of Aluminum Shape Casting Processing (San Antonio, Texas, USA) pp 143 – 52.
[4] Niyama E, Uchida T, Morikawa M and Saito S 1982 AFS Int. Cast Met. J. 7 52 – 63.
[5] Stefanescu D M 2005 Int. J. Cast Metal. Res. 18 129 – 43.

[6] Stefanescu D M 2009 Science and Engineering of Casting Solidification (New York, NY: Springer Science + Business Media).
[7] Carlson K D, Ou S, Hardin R A and Beckermann C 2002 Metall. Mater. Trans. A 33 731 – 40.
[8] Sigworth G K and Wang C 1993 Metall. Mater. Trans. B 24 349 – 64.
[9] Carlson K D and Beckermann C 2009 Metall. Mater. Trans. A 40 163 – 75.
[10] ESI Group 2013 ProCAST 2013.5: User's Manual (Paris: ESI Group).
[11] Nosir S. et al. Development of technology for obtaining quality castings from steel alloys //Eurasian Journal of Engineering and Technology. – 2022. – T. 5. – C. 135 – 138.
[12] Nosir S. et al. DEVELOPMENT OF QUALITY STEEL ALLOY LIQUIDATION TECHNOLOGY //American Journal of Interdisciplinary Research and Development. – 2022. – T. 7. – C. 74 – 83.
[13] Nosir S. et al. Improvement of Technology of Liquefaction of Gray Cast Iron Alloy //Global Scientific Review. – 2022. – T. 6. – C. 19 – 28.
[14] Saidmakhamadov N. M. et al. DEVELOPMENT OF TECHNOLOGY FOR LIQUEFACTION OF STEEL ALLOYS: DEVELOPMENT OF TECHNOLOGY FOR LIQUEFACTION OF STEEL ALLOYS. – 2023.
[15] Saidmakhamadov N. et al. IMPROVEMENT OF THE TECHNOLOGY OF CASTING SHAFT COMPONENTS FROM 35XGCL BRAND STEEL IN AN ELECTRIC ARC FURNACE //American Journal of Interdisciplinary Research and Development. – 2023. – T. 15. – C. 59 – 66.
[16] Saidmakhamadov N. et al. Improvement of liquidation technology of construction steels //Техника и технологии машиностроения. – 2022. – C. 57 – 62.
[17] Saidmakhamadov N. M. et al. Improve Casting Properties of Steel Alloy //Miasto Przyszłości. – 2023. – T. 40. – C. 323 – 328.
[18] Kholmirzaev N. et al. Effects of titanium (Ti) contents on the wear resistance of low-alloy steel alloys //E3S Web of Conferences. – EDP Sciences, 2024. – T. 525. – C. 03003.
[19] Saidmakhamadov N. et al. Improving the design of the lining of the ball mill used to improve the quality of grinding //E3S Web of Conferences. – EDP Sciences, 2024. – T. 525. – C. 02017.
[20] Saidmakhamadov N. M. et al. Energy Balance In Steel Liquefaction In Induction Furnaces And Electric Arc Furnaces //Academicia Globe: Inderscience Research. – 2023. – T. 1. – №. 2. – C. 9 – 9.